POLITECNICO DI TORINO
Repository ISTITUZIONALE

Multilayer plastic film chemical recycling via sequential hydrothermal liquefaction

(Article begins on next page)

12 June 2023

Multilayer plastic film chemical recycling via sequential hydrothermal liquefaction

Edoardo Tito [a], Juliano Souza dos Passos [b], Samir Bensaid [a], Raffaele Pirone [a], Patrick Biller [b,*]

[a] *Department of Applied Science and Technology, Politecnico di Torino, Corso Duca degli Abruzzi 24, 10129, Turin, Italy*
[b] *Biological and Chemical Engineering, Aarhus University, Hangøvej 2, DK-8200, Aarhus N, Denmark*

ARTICLE INFO

ABSTRACT

Multi-material layered plastic films are used in the food packaging industry due to their excellent properties; however they cannot be mechanically recycled. In this study, a two-stage hydrothermal liquefaction (HTL) process is proposed and tested for chemical recycling of a two-layer film made of LLDPE-PET. Experimental results showed that after a first subcritical stage at 325 °C, 94% of terephthalic acid (TPA) is recovered from the PET fraction as a solid and 47% of ethylene glycol in the aqueous phase. The unconverted PE was then used as feedstock for a subsequent supercritical HTL stage at 450 °C for 90 min, achieving mass yields of 47% and 29% in a naphtha-gasoline oil and in an alkane-rich gas, respectively. In conclusion, this work proved that a sequential HTL procedure can be used for chemical recycling of multilayer plastics, allowing the recovery of PET monomers to be recycled back to the PET industry and a paraffinic oil and hydrocarbon-rich gas phase that could be used as feedstock for steam cracking to produce virgin materials.

1. Introduction

The production of plastic has increased significantly since the 1950s, when large-scale production of polymers began. This trend is due to the versatility and low production costs of plastics. However, plastic waste generation has also increased at a similar rate (OECD 2022). The management of this large amount of waste has so far been ineffective, with 79 wt.% ending up in landfills or in the natural environment, both on land and at sea (OECD 2022; Geyer et al., 2017).

The plastic packaging sector is the largest contributor to plastic waste generation, responsible for almost half of all plastic waste (Geyer et al., 2017). Plastics are well suited for the packaging industry due to their lightweight, reducing transportation cost and the amount of end-of-life waste (Ncube et al., 2021). Up to 84% of synthetic polymers used in the packaging market are thermoplastics (Marsh, 2016). The most common types are high-density and low-density polyethylene (HDPE and LDPE), polypropylene (PP), polystyrene (PS), polyvinyl-chloride (PVC), and polyethylene terephthalate (PET) (Ncube et al., 2021). The different polymers are used due to the different properties of packaging, e.g. to protect/preserve food, and merchandise, ease of transport and handling, etc. (Marsh and Bugusu, 2007).

In the packaging industry, multi-layer films are popular due to their versatility. They are produced via co-extrusion (no binding agent) or lamination (requiring binding agents). Multilayer materials are estimated to constitute 26% of all flexible plastic packaging and 10% of the total plastic packaging market by weight (Ellen MacArthur Foundation 2015). The great advantage of using multi-material multilayer is the possibility to combine different functionalities required for the correct conservation and transport of sensitive products, usually foodstuffs, in very thin films. Multi-material films are typically formed by two to nine layers (Butler and Morris, 2016) depending on the required properties. These usually include food compatibility, mechanical strength, heat sealability, gas/aroma and moisture barrier (de M. Soares et al., 2022). Together with versatility, the intrinsic characteristic of having multiple layers leads to an increased difficulty to apply common mechanical recycling techniques, which in practice hinders almost entirely the recyclability of this type of material. Possible solutions to multilayer plastic recycling that have been suggested include chemical recycling via pyrolysis (Cabrera et al., 2022) and solvent based dissolution processes followed by mechanical recycling (Walker et al., 2020). Both of these entail serious difficulties; pyrolysis cannot deal with elevated levels of PET due to high gas formation (Li et al., 2021) and clogging issues (Li et al., 2022), while dissolution uses vast amounts of often toxic solvents, making large scale implementation difficult (Li et al., 2022). To

---

* Corresponding author.
  E-mail address: pbiller@bce.au.dk (P. Biller).

solve this issue of recycling multilayer films, we herein suggest an approach that selectively recycles different polymer types using chemical recycling via hydrothermal liquefaction.

For the chemical recycling of plastics, attention is growing towards hydrothermal liquefaction (HTL). HTL is a technology that has been studied for the conversion of different bio- and synthetic polymers into oil by reaction in hydrothermal environment (Li et al., 2022; Gollakota et al., 2018). The HTL behavior strongly depends on the polymeric chains and an effective depolymerization is only achieved for some (dos Passos et al., 2020). It is known that polymers with no heteroatoms in the carbon chain, such as polyolefins (LDPE, HDPE, PP) or PS, are inert in subcritical water condition (below 374 °C and 22.1 MPa) due to the absence of active sites for hydrolysis (Seshasayee and Savage, 2020). Under supercritical HTL conditions (>374 °C) however, they can be converted into oil with high yields (Seshasayee and Savage, 2020; Jin et al., 2020; M. Čolnik et al., 2021). On the other hand, condensation polymers (e.g. PET, nylon, polyurethane) containing heteroatoms are easily hydrolyzed in subcritical conditions to their starting monomers (Goto, 2009).

PET hydrolysis during HTL has been extensively studied in the literature and compared to other processes (methanolysis, acid and alkaline hydrolysis), has the advantage of being more efficient while working at less harsh conditions (Cao et al., 2022; M. Čolnik et al., 2021). Upon heating, PET starts to be hydrolyzed at 250 °C giving the two constituent monomers, namely terephthalic acid (TPA) and ethylene glycol (EG) (Cao et al., 2022; M. Čolnik et al., 2021). In particular, attention was given to TPA recovery, due to its high yield, stability and physical properties, which could enable efficient separation (Goto, 2009; M. Čolnik et al., 2021; Yamamoto et al., 1996). The hydrolysis kinetics is favored by increasing the operating temperature, and at around 300 °C and 30 min, an almost complete recovery of TPA was achieved (M. Čolnik et al., 2021). However, if supercritical conditions are approached, TPA recoveries are decreased due to TPA conversion to benzoic acid (M. Čolnik et al., 2021). Moreover, at temperatures high enough not to limit kinetics but not too high to lead to degradation of TPA, no interaction between PET and polyolefins (PP) was observed (Mahadevan Subramanya et al., 2022).

In the current study, we propose to apply a two-stage HTL process for the chemical recycling of mixed plastic waste. In the first stage, a subcritical step is used to recover monomers from condensation polymers, while the more recalcitrant polyolefins are left unconverted and used as feed in a sequential supercritical HTL step to be broken down into useful chemicals and fuels. Such a sequential HTL concept was performed to a specific case, using a commercial two-layer film made of LLDPE-PET. PE and PET belong to the polyolefin and condensation polymer family, respectively, and represent the two polymers most commonly found in multi-material multilayer films (Roosen et al., 2020).

2. Materials & methods

A commercial multilayer film made of LLDPE-PET was used as the feedstock and was cut into small pieces (~1 cm) before use. The film had a total thickness of 72 μm, where 12 μm of PET was on top of a 60 μm LLDPE layer.

The two-stage HTL process was carried out with a first reaction under subcritical conditions and a subsequent reaction under supercritical conditions. A basic block diagram depicting the overall work flow of the experimental methodology is shown in Fig. 1 while the supplementary electronic material describe the individual reaction steps in detail.

In the subcritical phase (325 °C, 20 min) the aim was to hydrolyze PET to its monomers, namely ethylene glycol (EG) and terephthalic acid (TPA). While EG is soluble in the aqueous phase, TPA is solid at ambient temperature and can be removed from the unreacted PE through alkaline extraction, where TPA is converted into a water soluble salt. After the first stage, the solid phase rich in PE was then used as the feedstock for the supercritical stage in fresh water. The aim of the second stage was the conversion of polyolefins into oil and gasses rich in monomer-like molecules. Different operating conditions (425–475 °C, 60–120 min) were tested for the conversion of PE by using pure LDPE. The analytical methodology of the different product phases and product separation procedures are described in detail in the electronic supplementary material.

3. Results and discussion

3.1. Feedstock composition

FTIR spectra of the feedstock showed that one side of the film was made of PE while the other side was made of PET (Figure S1). In Figure S2 the TGA and DSC of the PE-PET feedstock are shown. The lower shoulder around 392 °C is due to PET decomposition while the big peak at 441 °C is due to LLDPE decomposition. Compared to literature (Latifa et al., 2020; Dubdub and Al-Yaari, 2020) these peaks resulted at lower temperature due to the much lower heating rate used in this work. The weight composition based on TGA analysis of the multilayer film is shown in Table 1. The ashes could be attributed to pigments used as dyes, while the remainder could be attributed to other additives or
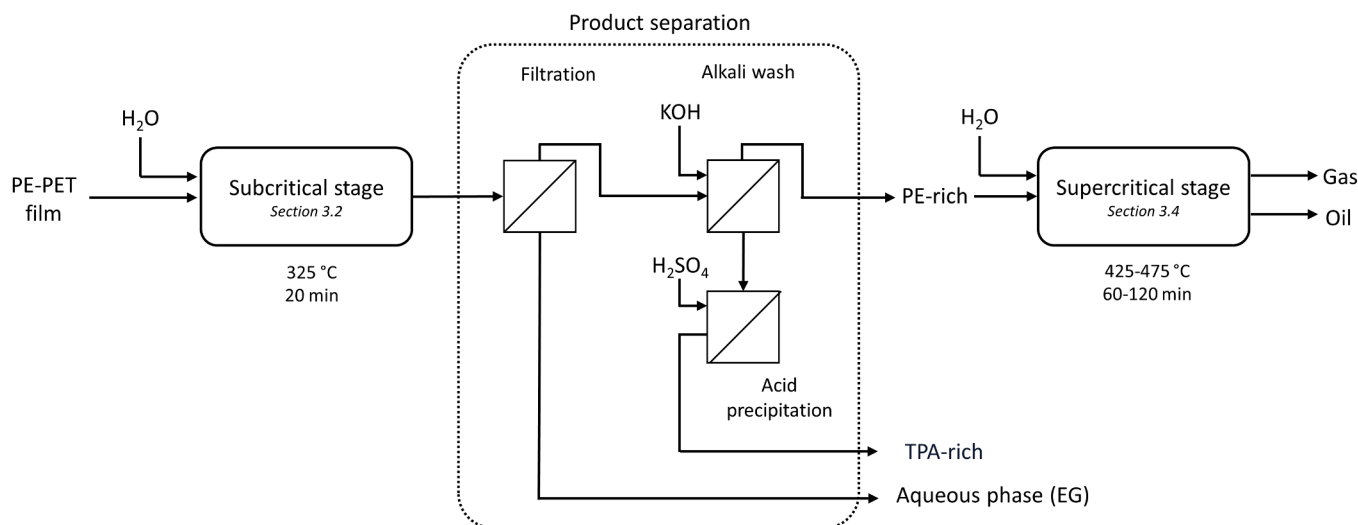

Fig. 1. Block diagram for the two-stage HTL.

Table 1
Multilayer composition evaluated by TGA.

	PET	PE	Other	Ash
Composition (wt.%)	17.2	73.0	8.3	1.5

adhesives (Li et al., 2022).

3.2. Subcritical stage

3.2.1. Mass yields

Fig. 2 shows the yields obtained after the subcritical stage at 325 °C for 20 min while in Figure S3 the two solid products, as well as the feedstock, are shown as photographs.

The PE-rich phase was the most produced product due to its higher initial amount compared to the other constituents. It is noteworthy that the yield of PE-rich phase was comparable to the initial amount of PE (Table 1). Its color shifted from blue of the starting film (Figure S3-A) to green-like (Figure S3-B); this change in color suggests a degradation of the colorant additives present in the starting feedstock. Almost all PE input in the first step was recovered in the PE-rich (98%) with high purity (96%) (Table 2). Polyolefins are well known to be recalcitrant in subcritical HTL due to the absence of heteroatoms in the structure (dos Passos et al., 2020). The same is observed here, as the PE melted under subcritical conditions and resolidified into a plastic cluster at room temperature.

The TPA-rich phase was recovered with a TPA purity of 78% and a TPA recovery of 94%. Some of the impurities present in the TPA-rich phase could be attributable to residual organics, as only 7% of the ash was detected in the TPA-rich phase by TGA. The TPA-rich phase showed a yellowish color (Figure S3-C) that differed from the white color of pure TPA. A difference in color was also observed by Mancini & Zanin between commercial TPA and TPA recovered after HTL treatment of post-consumer PET waste (Mancini and Zanin, 2004).

Simultaneously with the formation of TPA there should be an equimolar production of ethylene glycol (EG) from PET hydrolysis. However, the EG recovery in the aqueous phase was equal only to 47%. Yamamoto et al. were able to recover up to 70% of EG from PET with operating temperature between 250 °C and 300 °C (Yamamoto et al., 1996). Only 53% of the carbon registered in the AP was attributable to EG. The presence of other carbon in the AP other than the EG and the lower yields of EG compared with TPA is likely due to the fact that the EG is prone to be further degraded, forming mainly acetaldehyde,
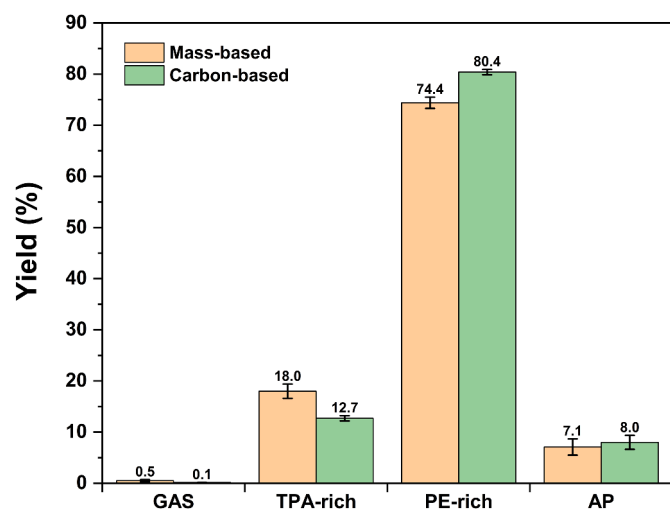
Table 2
Purity and yields for TPA-rich, PE-rich and AP obtained after subcritical stage. *EG quantified in the AP.

	TPA-rich	PE-rich	EG*
Purity (wt.%)	77.6 ± 4.5	96.1 ± 0.4	53.2 ± 16.9
Recovery (%)	94.1 ± 12.6	98.0 ± 1.8	47.3 ± 7.0

followed by 1,4-dioxane and diethylene glycol (Goto, 2009; M. Čolnik et al., 2021). 1,4-dioxane, acetaldehyde, benzoic acid and acetic acid concentration in the aqueous phase after reaction were estimated through GC-FID. However, apart from 1,4-dioxane (1.4 ± 0.2%), their carbon yields were negligible (<0.25%).

3.2.2. Elemental composition

In Fig. 3 the elemental analysis of feedstock, PE-rich and TPA-rich phases are reported. The multi-material multilayer film has a carbon-rich structure, comprising 78% carbon. This composition is quite similar to the theoretical elemental composition of a polymer consisting of 81 wt.% PE and 19 wt.% PET. The PE/PET ratio of 81/19 is the same that was evaluated for the multilayer film (73/17) in Table 1, without accounting for the remaining 10 wt.%. It follows that the discrepancies between the actual film and a theoretical film made only of PE and PET in the ratio 81/19 (PE81%-PET19%) are attributable to the 8.3 wt.% additives in the film. They consist of materials with a low carbon content and a higher oxygen content. The PE-rich phase has an elemental composition very close to the theoretical one of PE (Pure PE in Fig. 3) as suggested by its very high purity and yield (Table 2). However, it contains a slightly higher hydrogen concentration, resulting in a H/C molar ratio comparable with the theorical value (2.3 instead of 2.0), and not oxygenated. The absence of oxygen is interesting as it indicated that no residues from PET or TPA were left in the solid residue after alkali wash, and no oxygenation of PE took place during subcritical HTL. The elemental composition of the TPA-rich phase slightly differs from values obtained in previous studies from PET alone (dos Passos et al., 2020; Agostini et al., 2022), which were similar to the theoretical value for TPA (Pure TPA in Fig. 3). In this work, the hydrolysis of PET by HTL was carried out in the presence of polyolefins, which did not convert. For this reason, the solid TPA was present in the solid blob of melted polyolefins and had to be extracted through alkaline washings and then precipitate with a change in pH. On the other hand, the previously cited studies (dos Passos et al., 2020; Agostini et al., 2022) working with isolated PET,

Fig. 2. Mass yields obtained from the PE-PET multilayer after reaction at 325 °C for 20 min. Orange bars refer to mass-based yields, while green bars refer to carbon-based yields.
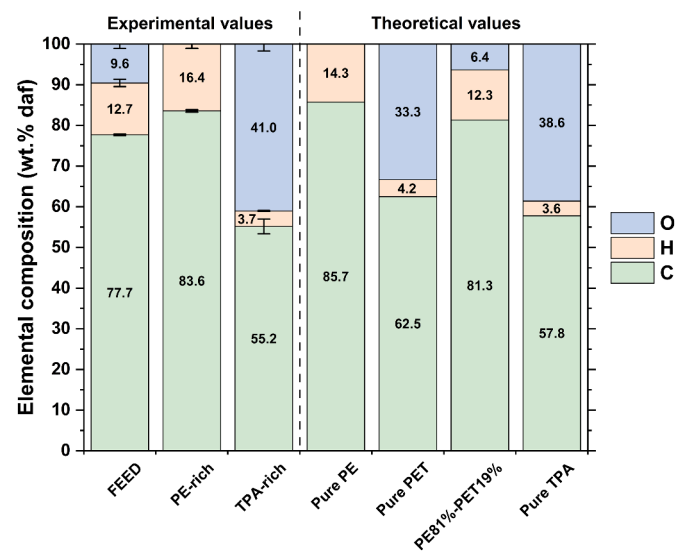

Fig. 3. Elemental analysis (daf basis) of feedstock and products from the subcritical stage (FEED, PE-rich, TPA-rich) and pure compounds used for comparison purposes (Pure PE, Pure PET, PE81%-PET19%, Pure TPA).

were able to obtain the purified TPA directly as a reaction product. It is therefore possible that the added stage used here slightly affected the elemental composition of the TPA-rich solid. It is worth noting that the alkaline wash used in this work to recover TPA was due to laboratory-scale experiments. In fact, the concept we propose would involve separation under subcritical conditions to recover TPA. On an industrial scale, hot water at about 250 °C is usually used to solubilize TPA (Zhou et al., 2006; Tomás et al., 2013), so a separation step under subcritical conditions would allow separation of the PE-rich solid phase from the purified TPA without the need for an alkali wash. The TPA-rich phase targeted during the subcritical step is similar to what is called crude TPA in petrochemistry (Tomás et al., 2013), which requires an additional purification step prior to polymerization in PET.

3.2.3. FTIR

The FTIR spectra of the PE-rich and TPA-rich solid are shown in Fig. 4. Looking at the PE-rich phase, some differences are evident compared with the PE-layer spectra. A new prominent peak appeared at 1430 cm^{-1} attributable to C—H bending vibration of -CH$_3$ groups, which usually has a medium intensity; it proves a consistent increase of methyl groups in the PE-rich phase that corroborates the higher H/C registered; it could be due to the hydrolysis of the chemical bonds present on the contact surface of the multilayer film. Another peak occurred at 880 cm^{-1}, attributed to geminal C—H bending vibration of alkenes (Silverstein et al., 1949). This peak is usually of strong intensity, while the other peaks generally attributed to alkenes are not visible, so it is possible that few alkene groups were formed within the solid. As observed from the elemental analysis, no oxygen-containing groups were detected. This result is in contrast to the previous work by dos Passos et al. (dos Passos et al., 2020), which observed the signal of carbonyl groups and no peak at 1430 cm^{-1} and 880 cm^{-1} in the solid obtained after HTL of pure HDPE and LDPE at 20 min at 350 °C. The absence of oxygen could be ascribed to the lower temperature (325 °C) used in this work, while the presence of methyl and olefinic groups could be attributed to the higher reactivity of the contact surface within the multilayer film requiring the recombination of the chemical bonds. The FTIR spectrum (Fig. 4) of TPA corresponds well to those reported in literature with pure TPA (Agostini et al., 2022; Yang et al., 2010), as well to the TPA standard analyzed for comparison purposes.

3.3. Screening of optimal conditions for PE conversion

Before performing the supercritical stage with the PE-rich sample recovered from the subcritical stage, a preliminary assessment with pure LDPE was carried out to find the optimal conditions of residence time and temperature. The experimental results obtained in every experiment are reported in Table S1, while the predictive models for oil and gas phase are given in Eq. (1) and Eq. (2). Temperature (T) is expressed in °C while residence time (t) is expressed in min. The analysis of variance (ANOVA) for oil and gas phase (Table S2–S3) show that the models are suited to explain the produced dataset. Additional diagnostic tests were performed to verify model bias and are illustrated in Figure S4–S5 for oil and gas yield models, respectively. The graphs show that all models are highly capable of predicting yields with a relatively low bias.

The contour plots resulting from the response surface methodology (RSM) are shown in Fig. 5. The oil yield showed a maximum with varying temperature and residence time (Fig. 5-A); in particular, temperature variations had the biggest influence on the oil yield, while the effect of residence time was most easily observed for higher temperatures (T > 450 °C). The strong dependence of HTL performances on temperature was expected, as it is well-known that temperature is the most important parameter for HTL (Mathanker et al., 2021; Akhtar and Amin, 2011). The maximum oil yield was predicted to be around 456 °C and 83 min, with an expected oil yield of 54%. Differences between experimental oil yields obtained at 450 °C, 90 min and 456 °C, 83 min were within the experimental errors (Table 3).

$$\text{Oil yield (wt.\%)} = -9.120 \cdot 10^3 + 3.9583 \cdot 10^1 \, T + 3.5148 \, t - 5.883 \cdot 10^{-3} \, tT \\ - 4.2847 \cdot 10^{-2} \, T^2 - 5.144 \cdot 10^{-3} \, t^2$$

(1)

$$\text{Gas yield (wt.\%)} = -9.0955 \cdot 10^2 + 3.7789 \, T - 1.6157 \, t + 2.967 \cdot 10^{-3} \, tT \\ - 3.724 \cdot 10^{-3} \, T^2 + 2.025 \cdot 10^{-3} \, t^2$$

(2)

At low temperatures (~ 425 °C), oil production is limited due to low conversion of LDPE, as observable from the high solid residue (Fig. 5-C). With increasing temperature, depolymerization is favored, resulting in increased oil. However, at the same time as the oil, the gas phase is also increased. Depolymerization of LDPE in supercritical water occurs
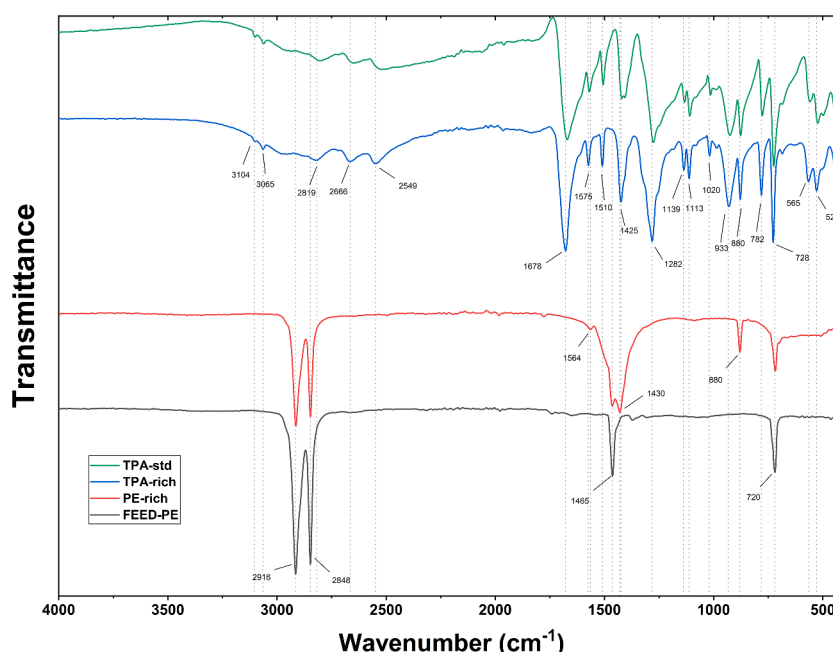

Fig. 4. FTIR spectra of TPA standard (green), TPA-rich phase (blue), PE-rich phase (red) and starting PE layer (black).
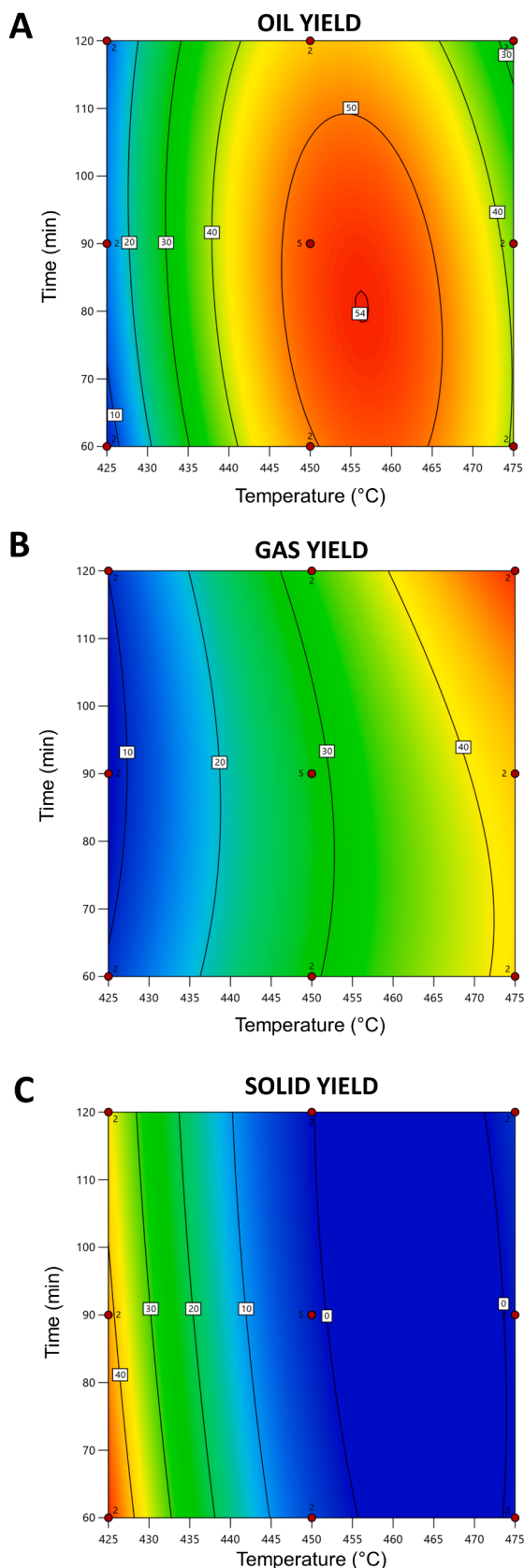
Fig. 5. Contour plots for oil (A), gas (B) and solid yield (C).

Table 3
Experimental yields obtained with pure LDPE.

	450 °C, 90 min	456 °C, 83 min
Oil yield (wt.%)	52.2 ± 4.1	49.1 ± 0.4
Gas yield (wt.%)	27.8 ± 0.9	34.0 ± 2.0
Solid yield (wt.%)	2.1 ± 0.2	0.3 ± 0.2

through free-radical random chain scission that leads to the formation of shorter hydrocarbon-like structures (Seshasayee and Savage, 2020). Depending on the ultimate length, these molecules under ambient conditions form solids, waxes ($C_n > 25$), liquids ($25 > C_n > 5$) or gasses ($C_n < 5$). At more severe conditions, the decomposition of hydrocarbons increasingly pronounced, leading to an increment of gaseous compounds that do not repolymerize. For this reason, the gas yield showed a constant upward trend with temperature (Fig. 5-B). Around 450–455 °C, the solid yield is almost zero while the yield in oil is highest, due to the trade-off between the decomposition of starting PE into oil and the further degradation of oil into gas. Residence time showed to have an effect only at temperatures higher than 450 °C. Under these conditions, an increase in reaction time strongly favors the conversion of oil primarily to gas.

Based on the RSM here discussed, the conditions of 450 °C and 90 min were chosen for the supercritical stage with the PE-rich phase.

3.4. Supercritical stage

3.4.1. Mass and carbon yields

The mass and carbon yields obtained under supercritical conditions (450 °C, 90 min) from the PE-rich phase are reported in Table 4. Yields using the PE-rich phase are similar to the ones obtained from pure LDPE (Table 3). It follows that the previous presence of PET in the multilayer did not have an impact on the reactivity of PE during the subsequent supercritical step. Surprisingly, the solid yield also closely matches the yield obtained from the pure sample. In fact, the real sample has an ash content of 1.9 ± 0.5 wt.%, which is probably the main reason for solid yields; hence a slightly higher solid yield would be expected. Alternatively, the ash could be solubilized in the aqueous phase or in the oil, as observed for Na, Ca, Mg (Panisko et al., 2015; Tito et al., 2022; Rizzo and Chiaramonti, 2022), some of the most common inorganic elements found in post-consumer plastic waste (Agostini et al., 2022). Due to the very low amount of solid produced, it was not possible to quantify the amount of ash present in the solid sample and its elemental composition. However, TGA analysis confirmed a limited ash content in the oil (lower than 400 ppm).

The carbon yield in the oil and gas phases during the PE-rich HTL are consistent with the mass yields. The sum of the carbon yields of gas and oil phases was found to be 76.2% (Table 4) while the remaining 23.8% was distributed among the other phases and losses during the work-up. As reported by Colnik et al. (M. Čolnik et al., 2021), the carbon yield in the aqueous phase for PE processing at similar conditions is less than 0.6%, and the carbon yield in the solid phase was also low due to the low mass yield reported here. Hence, it is likely that the missing portion is due to losses during the work-up, as volatile hydrocarbons found in oil and gas phases were easily lost due to very low boiling points.

3.4.2. Gas composition

The gas phase is composed of short hydrocarbons, as can be seen

Table 4
Mass and carbon yields obtained from the PE-rich phase at 450 °C for 90 min. The difference between 100 and the sum of the phases is also represented.

	Gas	Oil	Solid	Difference
Mass yield (wt.%)	28.9 ± 2.0	46.8 ± 4.7	2.1 ± 1.5	22.1 ± 8.2
Carbon yield (C%)	27.3 ± 6.3	48.9 ± 5.5	NQ	23.8 ± 11.8

from the gas composition reported in Table S4. Methane is the most abundant gas, accounting for almost a third of the total gas, while 79% of the total composition is made up of normal linear saturated alkanes. In addition, 6.5 vol.% of H_2 and 2.0 vol.% of CO_2 were identified. The presence of CO_2 is connected to the fact that the atmosphere inside the reactor was not inert before the reaction, resulting in oxidation of hydrocarbons by the residual oxygen. This can be further substantiated by the fact that the amount of CO_2 produced after reaction corresponds to the molar amount of oxygen left in the reactor before the reaction. It is hence possible to conclude that in the industrial implementation of this concept, there will be no CO_2 and that the higher heating value of the generated gas would be slightly higher than the 50.2 MJ/kg (60.8 MJ/Nm^3) calculated here.

3.4.3. Oil elemental composition

The oil phase was the highest yielding product, reaching 47 wt.% of the starting feedstock. Most of the oil (~90%) was recovered directly after the centrifugation of the liquid contained in the reactor (Figure S6), while the rest was collected through extraction with acetone. The oil was a very dark-brown liquid, with low viscosity and high volatility (Figure S6). The elemental composition was 87.3 ± 0.7% C and 12.7 ± 0.2% H, resulting in the empirical formula $C_nH_{1.7n}$. No oxygen was found, meaning that no oxygen from water is incorporated in the oil, as would be expected from the thermal decomposition through free-radical chain scission of polyethylene (Zhao et al., 2021). However, the oxygen content was evaluated by difference from the carbon and hydrogen contents and an uncertainty of ± 1% is associated to its quantification. Slightly higher values were estimated by Lu et al. (2022), obtaining an oil with 2.3 wt.% oxygen after HTL at 450 °C for 4 h from HDPE (Lu, 2022), while Chen et al. converted polypropylene at the same conditions used in this work obtaining an oil with less than 0.6 wt.% of oxygen (Chen et al., 2019). The HHV of the oil was evaluated as 45.4 MJ/kg, hence in the range of diesel. As also observed in literature (Seshasayee and Savage, 2020; Lu, 2022; Chen et al., 2019), the oil produced from supercritical HTL of polyolefins has a very high heating value that makes it suitable not only as fuel but also as a feedstock for chemical production. The advantage in HTL oil quality from polyolefins stands out when comparing the HHV with HTL oils obtained from biomass (Gollakota et al., 2018).
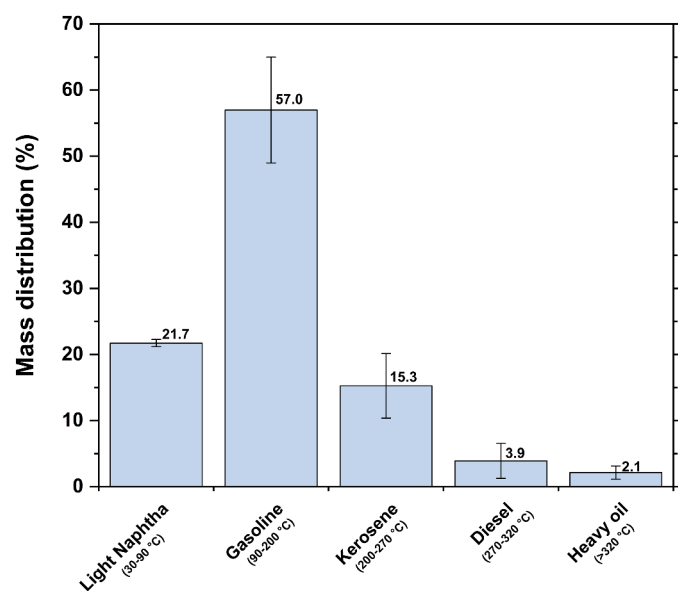
3.4.4. Boiling point

The boiling point distribution of the oil assessed by TGA is shown in Fig. 6. The boiling points were divided into light naphtha (30–90 °C), gasoline (90–200 °C), kerosene (200–270 °C), diesel (270–320 °C) and heavy oil (>320 °C). Most of it was in the naphtha-gasoline range, making its use as a steam cracker feedstock, since this is the predominant feedstock used for steam cracking in Europe and Asia (Ullmann's 2000). The high gas yield registered in Table 4 is hence explained by the fact that the PE was cracked down into small molecules with carbon number lower than 12 and that, according to their boiling points, ended up as part of the gas or oil phase. However, it is very likely that the amount of naphtha was underestimated due to losses during work-up, favored by the low amount of feedstock used for the reaction, which led to the missing mass in Fig. 6, and during the TGA, as the high volatility was clearly visible, leading to the underestimation of light naphtha. A similar boiling point distribution was also observed by Lu et al. after supercritical HTL of HDPE-based plastic waste at 450 °C for 4 h (Lu, 2022).

3.4.5. FTIR and oil composition via GC–MS

FTIR of the oil phase is reported in Figure S7. The main peaks are attributable to a linear paraffinic structure. That is, alkane C—H stretching within 2955–2854 cm^{-1}, methylene C—H bending at 1455 cm^{-1}, methyl C—H bending at 1377 cm^{-1}, methylene C—H rocking at 725 cm^{-1} (Mirghani and Che Man, 2003; Bucci et al., 2015). The GC–MS spectrum of the oil is shown in Figure S8 while the chemical composition of the oil phase, expressed as the ratio of peak area to total integrated area and differentiated by carbon number, is reported in Fig. 7. The highest peak is associated to C8 compounds and 79% of the total chromatogram area is related to compounds with carbon number ranging from 7 to 12. The concentration of these compounds is mainly related to the large amount of aromatics recorded in this range. Most of them are alkylbenzenes, while a smaller part at higher carbon numbers is due to indane derivatives. Overall, from the ratio between peak areas, aromatics and n-paraffins represent the two most present group of molecules. Polycyclic aromatic hydrocarbons (PAHs) were mostly observed as alkylated derivatives of naphthalene, the simplest PAH. Cyclic paraffins were most favored at low carbon number, while isoparaffins were very low. Olefins and cyclic olefins were recorded in smaller quantities than paraffins.

Although the ratio of peak area to total integrated area is usually used in literature to study the composition of oil from HTL, a
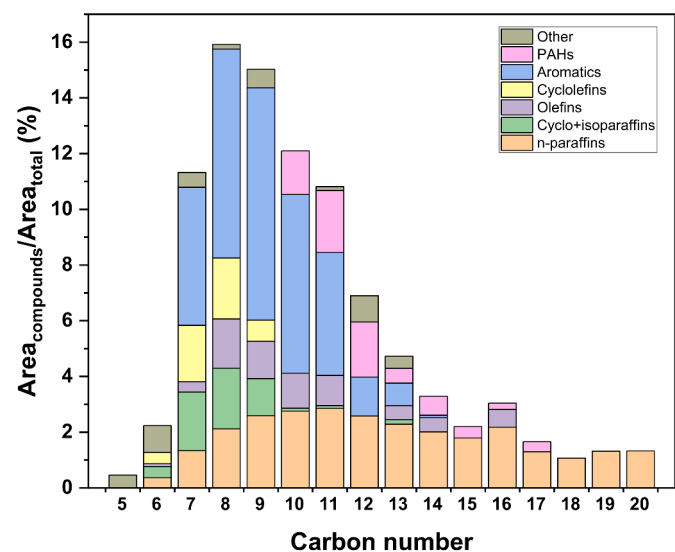

Fig. 6. Boiling point distribution of the oil. Boiling points range: light naphtha 30–90 °C, gasoline 90–200 °C, kerosene 200–270 °C, diesel 270–320 °C and heavy oil >320 °C.

Fig. 7. Composition of oil obtained after HTL at 450 °C for 90 min from the PE-rich phase. Data are expressed as a percentage of the area of each compound compared to the total integrated area.

quantification of the present compounds should be performed through external calibrations. From the calibrations, the overall concentration of n-paraffins (C6-C31), aromatics (BTEX and some isomers) and PAHs amounted to 30.9 ± 2.5, 9.4 ± 2.2 and 3.0 ± 0.7 wt.%. n-paraffins confirmed to be present in a high extent in the oil but, as can be seen from Fig. 8, the carbon distribution was shifted towards lower values than those shown in Fig. 7. The amount of aromatics appeared limited compared to Fig. 7, also due to the limited amount of compounds tested, especially indane-derivatives. In Table S6 is reported the quantification of all the calibrated compounds.

The conversion of PE during supercritical HTL occurs through a random chain scission that converts the polymer into linear radical chains (Zhao et al., 2021). These free-radical fragments are subsequently converted via β-scission into olefins plus smaller radicals, which can react with other radical fragments to form linear paraffins (Jin et al., 2020). The formation of olefins by β-scission is confirmed in this work by the fact that almost all olefins identified by GC–MS are α-olefins. Paraffins can then be further reduced in size through the same mechanisms, up to the point of forming gaseous compounds; olefins, on the other hand, tend to polymerize forming cyclic structure that eventually can produce more stable aromatics through dehydrogenation (Zhao et al., 2021). The occurrence of these pathways is confirmed by the high amount of linear alkanes, the low concentration of isoalkanes, the presence of olefins, cyclic compounds and aromatics. Moreover, the high amount of aromatics, along with the limited amount of olefins in both oil and gas phase, and the low boiling point of the oil confirm a high progress within the pathway.

The paraffinic-rich composition of the oil, together with a higher amount of n-paraffins than isoparaffins and a naphtha-like boiling point, makes it an interesting feedstock for steam cracking, as well as the paraffinic gas phase (Gholami et al., 2021). Thus, olefins needed for virgin polymer production could be produced from this recycled oil phase. Kusenberg et al. tested the use of pyrolysis oil obtained from PE film as feedstock to steam cracking in co-feeding with fossil naphtha (M. Kusenberg et al., 2022). Ethylene production and char formation were higher than those obtained from fossil naphtha alone. However, compared to the HTL-derived oil obtained in this work, the pyrolysis-derived oil from PE has a higher boiling point that gave it a wax-like appearance (M. Kusenberg et al., 2022; M. Kusenberg et al., 2022). Kusenberg et al. hence also proved the possibility of using the naphtha fraction obtained after the distillation of pyrolysis oil from real plastic waste as the sole feedstock for steam cracking (M. Kusenberg
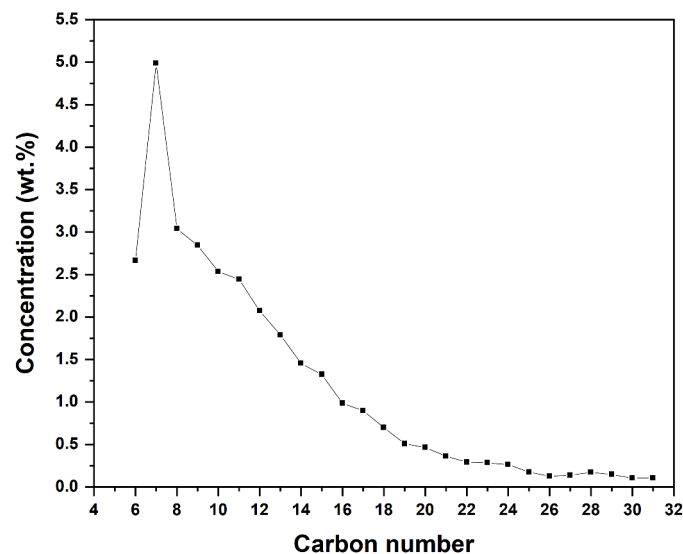
et al., 2022). Despite some differences in the composition of the oils, in particular the higher presence of unsaturated compounds in pyrolysis oil, the naphtha fraction obtained from pyrolysis oil should be closer to the oil obtained in this work. For this reason, good performance in steam cracking is likely with the oil produced through HTL.

3.5. Overall performances

Fig. 9 shows the mass distribution to the different phases after the subcritical and supercritical stages. As described earlier in Section 3.2.1, following the subcritical stage, the mass yields among the phases quite accurately reflect the initial composition of the multilayer film. Hence, it is reasonable to assume if the feedstock was changed to a film with different proportions of PE-PET, that the mass distribution would change accordingly. After conversion of the PE-rich in the supercritical stage, a gas phase, an oil and a low amount of residual solid are obtained.

The overall yields from the starting feedstock are 21.5 wt.% and 34.8 wt.% for the gas and oil phase, respectively, while their overall energy recoveries are 26.8% and 39.2%. Moreover, the losses in the Sankey diagram, are as discussed previously more than likely light hydrocarbons lost during the sample work-up procedure. For this reason, it is likely that up to 72.8% of the mass of the starting feedstock ends up as gaseous/oily hydrocarbons. In terms of chemical recycling, these streams could be used in the petrochemical industry as feedstock for a steam cracker to produce new olefins. Indeed, 63 wt.% of the light hydrocarbons forming the gas phase are alkanes, excluding CH_4, which are suitable for conversion into olefins. On the other hand, the lighter portion of the gas phase could be separated to have a stream of CH_4 and H_2 that could be burnt (2 MJ/kg film) to partially meet the thermal energy demand of the plant. Concerning the oil, at least 31 wt.% of it is formed by n-paraffins (mainly C6-C15), making it an interesting feedstock for steam cracking.

From the subcritical step, 18 wt.% of the multilayer film has been converted into a TPA-rich phase. It is worth emphasizing that, while in this work an alkali wash was necessary to separate the TPA-rich phase from the melted PE-rich phase, given the lab scale, in an industrial implementation of this process the separation would be engineered to be performed directly under subcritical conditions. Indeed, TPA is soluble in subcritical water (Takebayashi et al., 2012), and a separation under these conditions would be more efficient, economical, and environmentally friendly. However, the subcritical separation process needs to be further studied and optimized in-depth. For this reason, although the TPA purity in the TPA-rich phase was 78 wt.%, this value could be affected by the separation technology used. The TPA-rich product can be then used by the petrochemical industry has a raw material for the production of TPA, limiting the use of fossil sources. Besides TPA, EG, PET's other monomer, is also produced by the HTL sequential process. However, EG is found in the aqueous phase obtained after the subcritical stage at a concentration close to 1 wt.% together with other water-soluble compounds. As with TPA, EG could be recycled in the PET industry, provided that recovery from the water stream is not excessively expensive.

4. Conclusions

This study presented a two-stage HTL process for chemical recycling of multi-material multilayer plastic films. The study is carried out using a LLDPE-PET film but the concept can likely be expanded to many if not most multi-material plastic films. Through the first subcritical stage, it is possible to completely hydrolyze PET and recover its monomers, namely terephthalic acid (TPA) and ethylene glycol. The residual polyolefin did not show any substantial degradation after the first stage, it just melted and resolidified after cooling. The residual PE can be valorized by the second HTL stage under supercritical conditions. At the optimized operating conditions of 450 °C and 90 min it is possible to completely
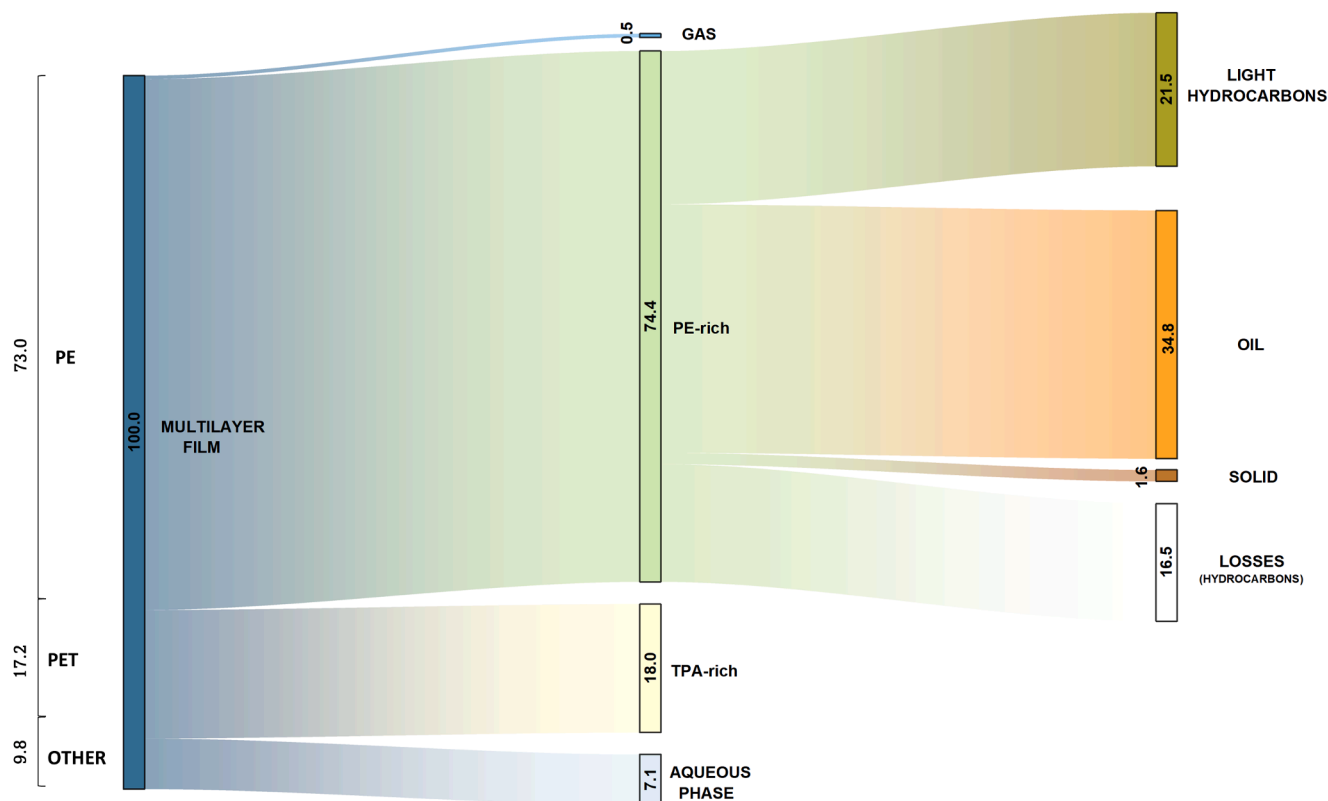

Fig. 8. n-paraffins concentration (wt.%) in the oil obtained after HTL at 450 °C for 90 min from the PE-rich phase.

Fig. 9. Mass distribution between the different phases after subcritical (325 °C, 20 min) and supercritical stages (450 °C, 90 min).

convert all the PE by obtaining a gas and oil phase. The gas phase consists mostly of saturated alkanes, and can be used as feedstock for steam cracking to produce olefins required by the plastics industry. In this way, a chemical recycling loop would be created. The oil phase has a boiling point distribution comparable to light naphtha-gasoline, a composition rich in n-paraffins and aromatics and no oxygenation. For the technical implementation of this technology, further research should be conducted for the integration of the two stages (subcritical and supercritical) from a thermal and product separation perspective.

CRediT authorship contribution statement

Edoardo Tito: Investigation, Methodology, Formal analysis, Writing – original draft, Visualization. **Juliano Souza dos Passos:** Conceptualization, Methodology, Investigation, Supervision, Writing – review & editing. **Samir Bensaid:** Supervision. **Raffaele Pirone:** Supervision. **Patrick Biller:** Conceptualization, Writing – review & editing, Resources, Supervision, Funding acquisition.

Declaration of Competing Interest

The authors declare that they have no known competing financial interests or personal relationships that could have appeared to influence the work reported in this paper.

Data availability

Data will be made available on request.

Acknowledgments

Supplementary materials

Supplementary material associated with this article can be found, in the online version, at doi:10.1016/j.resconrec.2023.107067.

References

Agostini, I., Ciuffi, B., Gallorini, R., Rizzo, A.M., Chiaramonti, D., Rosi, L., 2022. Recovery of terephthalic acid from densified post-consumer plastic mix by HTL process. Molecules 27. https://doi.org/10.3390/molecules27207112.

Akhtar, J., Amin, N.A.S., 2011. A review on process conditions for optimum bio-oil yield in hydrothermal liquefaction of biomass. Renew. Sustain. Energy Rev. 15, 1615–1624. https://doi.org/10.1016/j.rser.2010.11.054.

Bucci, R., Girelli, A.M., Tafani, S., Tarola, A.M., 2015. Oils and grease determination by FT-IR and n-hexane as extraction solvent. J. Anal. Chem. 70, 316–319. https://doi.org/10.1134/S106193481503017X.

T.I. Butler, B.A. Morris, PE-based multilayer film structures, in: multilayer flex. Packag. Second Ed., 2016: pp. 281–310. https://doi.org/10.1016/B978-0-323-37100-1.00017-X.

Cabrera, G., Li, J., Maazouz, A., Lamnawar, K., 2022. A journey from processing to recycling of multilayer waste films: a review of main challenges and prospects. Polymers (Basel) 14. https://doi.org/10.3390/polym14122319.

Cao, F., Wang, L., Zheng, R., Guo, L., Chen, Y., Qian, X., 2022. Research and progress of chemical depolymerization of waste PET and high-value application of its depolymerization products. RSC Adv. 12, 31564–31576. https://doi.org/10.1039/d2ra06499e.

Chen, W.T., Jin, K., Linda Wang, N.H., 2019. Use of supercritical water for the liquefaction of polypropylene into oil. ACS Sustain. Chem. Eng. 7, 3749–3758. https://doi.org/10.1021/acssuschemeng.8b03841.

Čolnik, M., Knez, Ž., Škerget, M., 2021b. Sub- and supercritical water for chemical recycling of polyethylene terephthalate waste. Chem. Eng. Sci. 233 https://doi.org/10.1016/j.ces.2020.116389.

Čolnik, M., Kotnik, P., Knez, Ž., Škerget, M., 2021a. Hydrothermal decomposition of polyethylene waste to hydrocarbons rich oil. J. Supercrit. Fluids. 169 https://doi.org/10.1016/j.supflu.2020.105136.

de M. Soares, C.T., Ek, M., Östmark, E., Gällstedt, M., Karlsson, S., 2022. Recycling of multi-material multilayer plastic packaging: current trends and future scenarios. Resour. Conserv. Recycl. 176, 105905 https://doi.org/10.1016/J.RESCONREC.2021.105905.

dos Passos, J.S., Glasius, M., Biller, P., 2020. Screening of common synthetic polymers for depolymerization by subcritical hydrothermal liquefaction. Process Saf. Environ. Prot. 139, 371–379. https://doi.org/10.1016/j.psep.2020.04.040.

Dubdub, I., Al-Yaari, M., 2020. Pyrolysis of low density polyethylene: kinetic study using TGA data and ANN prediction. Polymers (Basel) 12. https://doi.org/10.3390/POLYM12040891.

Ellen MacArthur Foundation, The new plastics economy: catalysing action, 2015. https://ellenmacarthurfoundation.org/the-new-plastics-economy-catalysing-action.

Geyer, R., Jambeck, J.R., Law, K.L., 2017. Production, use, and fate of all plastics ever made. Sci. Adv. 3, 3–8. https://doi.org/10.1126/sciadv.1700782.

Gholami, Z., Gholami, F., Tišler, Z., Vakili, M., 2021. A review on the production of light olefins using steam cracking of hydrocarbons. Energies 14, 1–24. https://doi.org/10.3390/en14238190.

Gollakota, A.R.K., Kishore, N., Gu, S., 2018. A review on hydrothermal liquefaction of biomass. Renew. Sustain. Energy Rev. 81, 1378–1392. https://doi.org/10.1016/j.rser.2017.05.178.

Goto, M., 2009. Chemical recycling of plastics using sub- and supercritical fluids. J. Supercrit. Fluids. 47, 500–507. https://doi.org/10.1016/j.supflu.2008.10.011.

Jin, K., Vozka, P., Kilaz, G., Chen, W.T., Wang, N.H.L., 2020. Conversion of polyethylene waste into clean fuels and waxes via hydrothermal processing (HTP). Fuel 273, 117726. https://doi.org/10.1016/j.fuel.2020.117726.

Kusenberg, M., Faussone, G.C., Thi, H.D., Roosen, M., Grilc, M., Eschenbacher, A., De Meester, S., Van Geem, K.M., 2022c. Maximizing olefin production via steam cracking of distilled pyrolysis oils from difficult-to-recycle municipal plastic waste and marine litter. Sci. Total Environ. 838, 156092 https://doi.org/10.1016/j.scitotenv.2022.156092.

Kusenberg, M., Roosen, M., Zayoud, A., Djokic, M.R., Dao Thi, H., De Meester, S., Ragaert, K., Kresovic, U., Van Geem, K.M., 2022a. Assessing the feasibility of chemical recycling via steam cracking of untreated plastic waste pyrolysis oils: feedstock impurities, product yields and coke formation. Waste Manag. 141, 104–114. https://doi.org/10.1016/j.wasman.2022.01.033.

Kusenberg, M., Zayoud, A., Roosen, M., Thi, H.D., Abbas-Abadi, M.S., Eschenbacher, A., Kresovic, U., De Meester, S., Van Geem, K.M., 2022b. A comprehensive experimental investigation of plastic waste pyrolysis oil quality and its dependence on the plastic waste composition. Fuel Process. Technol. 227, 107090 https://doi.org/10.1016/j.fuproc.2021.107090.

Latifa, B., Zohra, F.F., Said, H., 2020. Study of raw and recycled polyethylene terephthalate by meaning of TGA and computer simulation. Adv. Polym. Technol. 2020 https://doi.org/10.1155/2020/8865926.

Li, H., Aguirre-villegas, H.A., Allen, R.D., Bai, X., Benson, C.H., 2022. Expanding plastics recycling technologies : chemical aspects, technology status and challenges. Green Chem. 8899–9002. https://doi.org/10.1039/D2GC02588D.

Li, S., Cañete Vela, I., Järvinen, M., Seemann, M., 2021. Polyethylene terephthalate (PET) recycling via steam gasification – The effect of operating conditions on gas and tar composition. Waste Manag. 130, 117–126. https://doi.org/10.1016/J.WASMAN.2021.05.023.

Lu, T., 2022. Hydrothermal liquefaction of pretreated polyethylene-based ocean-bound plastic waste in supercritical water. J. Energy Inst., 141267 https://doi.org/10.1016/j.joei.2022.10.003.

Mahadevan Subramanya, S., Mu, Y., Savage, P.E., 2022. Effect of cellulose and polypropylene on hydrolysis of polyethylene terephthalate for chemical recycling. ACS Eng. Au. https://doi.org/10.1021/acsengineeringau.2c00024.

Mancini, S.D., Zanin, M., 2004. Optimization of neutral hydrolysis reaction of post-consumer PET for chemical recycling. Prog. Rubber, Plast. Recycl. Technol. 20, 117–132. https://doi.org/10.1177/147776060402000202.

Marsh, K., Bugusu, B., 2007. Food packaging - Roles, materials, and environmental issues: scientific status summary. J. Food Sci. 72 https://doi.org/10.1111/j.1750-3841.2007.00301.x.

Marsh, K.S., 2016. Polymer and plastic packaging. Ref. Modul. Food Sci. https://doi.org/10.1016/b978-0-08-100596-5.03379-5. Elsevier.

Mathanker, A., Das, S., Pudasainee, D., Khan, M., Kumar, A., Gupta, R., 2021. A review of hydrothermal liquefaction of biomass for biofuels production with a special focus on the effect of process parameters, co-solvents and extraction solvents. Energies 14, 4916. https://doi.org/10.3390/en14164916.

Mirghani, M.E.S., Che Man, Y.B., 2003. Determination of hexane residues in vegetable oils with FTIR spectroscopy. JAOCS, J. Am. Oil Chem. Soc. 80, 619–623. https://doi.org/10.1007/s11746-003-0748-3.

Ncube, L.K., Ude, A.U., Ogunmuyiwa, E.N., Zulkifli, R., Beas, I.N., 2021. An overview of plasticwaste generation and management in food packaging industries. Recycling 6, 1–25. https://doi.org/10.3390/recycling6010012.

OECD, 2022. Global Plastics Outlook: Economic Drivers, Environmental Impacts and Policy Options. OECD Publishing, Paris. https://doi.org/10.1787/de747aef-en.

Panisko, E., Wietsma, T., Lemmon, T., Albrecht, K., Howe, D., 2015. Characterization of the aqueous fractions from hydrotreatment and hydrothermal liquefaction of lignocellulosic feedstocks. Biomass and Bioenergy 74, 162–171. https://doi.org/10.1016/j.biombioe.2015.01.011.

Rizzo, A.M., Chiaramonti, D., 2022. Blending of hydrothermal liquefaction biocrude with residual marine fuel: an experimental assessment. Energies 15, 450. https://doi.org/10.3390/en15020450.

Roosen, M., Mys, N., Kusenberg, M., Billen, P., Dumoulin, A., Dewulf, J., Van Geem, K.M., Ragaert, K., De Meester, S., 2020. Detailed analysis of the composition of selected plastic packaging waste products and its implications for mechanical and thermochemical recycling. Environ. Sci. Technol. 54, 13282–13293. https://doi.org/10.1021/acs.est.0c03371.

Seshasayee, M.S., Savage, P.E., 2020. Oil from plastic via hydrothermal liquefaction: production and characterization. Appl. Energy. 278, 115673 https://doi.org/10.1016/j.apenergy.2020.115673.

R.M. Silverstein, F.X. Webster, D.J. Kiemle, Spectrometric identification of organic compounds (seventh edition), 1949.

Takebayashi, Y., Sue, K., Yoda, S., Hakuta, Y., Furuya, T., 2012. Solubility of terephthalic acid in subcritical water. J. Chem. Eng. Data. 57, 1810–1816. https://doi.org/10.1021/je300263z.

Tito, E., Zoppi, G., Pipitone, G., Miliotti, E., Di Fraia, A., Rizzo, A.M., Pirone, R., Chiaramonti, D., Bensaid, S., 2022. Conceptual design and techno-economic assessment of coupled hydrothermal liquefaction and aqueous phase reforming of lignocellulosic residues. J. Environ. Chem. Eng., 109076 https://doi.org/10.1016/J.JECE.2022.109076.

Tomás, R.A.F., Bordado, J.C.M., Gomes, J.F.P., 2013. P-xylene oxidation to terephthalic acid: a literature review oriented toward process optimization and development. Chem. Rev. 113, 7421–7469. https://doi.org/10.1021/cr300298j.

Ullmann's Encyclopedia of industrial chemistry, 2000. https://doi.org/10.1002/14356007.

Walker, T.W., Frelka, N., Shen, Z., Chew, A.K., Banick, J., Grey, S., Kim, M.S., Dumesic, J.A., Van Lehn, R.C., Huber, G.W., 2020. Recycling of multilayer plastic packaging materials by solvent-targeted recovery and precipitation. Sci. Adv. 6, 1–10. https://doi.org/10.1126/sciadv.aba7599.

Yamamoto, S., Aoki, M., Yamagata, M., 1996. Recovery of monomers from polyethylene terephthalate by hydrolysis under pressure. R D Kobe Seiko Giho 46, 60–63.

Yang, Z., Peng, H., Wang, W., Liu, T., 2010. Kinetics of neutral hydrolytic depolymerization of PET (Polyethylene Terephthalate) waste at higher temperature and autogenious pressures. J. Appl. Polym. Sci. 116, 2658–2667, 10.1002/app.

Zhao, P., Yuan, Z., Zhang, J., Song, X., Wang, C., Guo, Q., Ragauskas, A.J., 2021. Supercritical water co-liquefaction of LLDPE and PP into oil: properties and synergy. Sustain. Energy Fuels. 5, 575–583. https://doi.org/10.1039/d0se01486a.

Zhou, J.H., Shen, G.Z., Zhu, J., Yuan, W.K., 2006. Terephthalic acid hydropurification over Pd/C catalyst. Stud. Surf. Sci. Catal. 159, 293–296. https://doi.org/10.1016/s0167-2991(06)81591-0.